ISSN 2411-3336; e-ISSN 2541-9404

JOURNAL OF MINING INSTITUTE
Zapiski Gornogo instituta
Journal homepage: pmi.spmi.ru

Research article
Geotechnical Engineering and Engineering Geology

Analysis of the influence of viscoelastic properties of a synthetic hydraulic fracturing fluid on proppant transport capacity

Dinis V. Imangulov✉, **Aleksandr I. Ponomarev**, **Denis V. Kashapov**
Ufa State Petroleum Technological University, Ufa, Republic of Bashkortostan, Russia

***How to cite this article*:** Imangulov D.V., Ponomarev A.I., Kashapov D.V. Analysis of the Influence of viscoelastic properties of a synthetic hydraulic fracturing fluid on proppant transport capacity. Journal of Mining Institute. 2026. Vol. 279, p. 70-81.

Abstract

One of the pressing scientific challenges in the field of hydrocarbon production enhancement from hard-to-recover reserves using hydraulic fracturing is the insufficient understanding of how the elastic properties of hydraulic fracturing fluids affect proppant retention efficiency during fracture initiation in the near-wellbore zone. Earlier domestic and foreign studies on proppant transport capacity assert that fluid viscosity plays a key role in proppant retention; however, recent data indicate a significant influence of the elastic properties of polymer systems, particularly when using low-viscosity synthetic hydraulic fracturing fluids based on polyacrylamide (PAM). This study aims to provide a fundamental substantiation of the effect of viscoelastic properties of hydraulic fracturing fluids on proppant transport efficiency. The article presents the methodology and results of laboratory tests evaluating the viscoelastic and proppant transport properties of PAM-based and guar polymer-based hydraulic fracturing fluids. The findings demonstrate that PAM-based hydraulic fracturing fluids, despite their low effective system viscosity, exhibit more pronounced elastic properties compared to linear guar gels: the relaxation time and the first normal stress difference for the synthetic hydraulic fracturing fluid are 1.99 and 4 times greater than the corresponding values for the linear guar gel. The test results confirmed that the proppant settling rate in the PAM-based hydraulic fracturing fluid under static conditions was 28 times lower than that in the linear guar gel at equivalent active substance concentrations. The elastic properties of hydraulic fracturing fluids have a substantial effect on proppant transport capacity, supporting the potential of using low-viscosity synthetic PAM-based hydraulic fracturing fluids to enhance hydrocarbon production from reservoirs with permeability less than 1 mD.

Keywords

rheology; viscoelastic properties; hydraulic fracturing fluid; polyacrylamide; proppant transport capacity; relaxation time; first normal stress difference

Funding

None.

Received: 06.05.2025 ***Accepted: 04.03.2026*** ***Online: 18.05.2026***

Introduction

Hydraulic fracturing is one of the most widely applied methods for enhanced oil recovery and production stimulation. The concept involves injecting a treatment fluid (hydraulic fracturing fluid) into the target formation at a pressure exceeding the mechanical strength limit of the rock. As a result, a fracture is initiated in the near-wellbore region. To prevent fracture closure after pressure release and before well startup, a proppant – ceramic proppant or quartz sand – is used [1]. For the planned volume of proppant to fill the fracture interior and maintain permeability, the hydraulic fracturing fluid must possess specific technological properties that depend on its rheology [2].

Developed innovative synthetic hydraulic fracturing fluids based on polyacrylamide (PAM), in contrast to standard crosslinked guar-borate fluids, exhibit pronounced elasticity with significantly lower system viscosity (Fig.1) [3]. The use of these fluids makes it possible to bring into production hard-to-recover hydrocarbon reserves in reservoirs with permeability less than 1 mD [4].

Early studies [5, 6] on the physicochemical properties of hydraulic fracturing fluids asserted that fluid viscosity plays a key role in proppant retention and transport processes. However, recent research [7, 8] indicates a significant influence of elastic properties on the proppant transport capacity of the fluid.

Specifically, study [9] presented an investigation into the effect of elastic properties of hydraulic fracturing fluids based on anionic PAM prepared in distilled water on the proppant settling rate, using single quartz particles as the proppant. The study was conducted under static conditions at a temperature of 25 °C. Freshly prepared PAM-based hydraulic fracturing fluid samples with concentrations of 3; 5, and 9 l/m^3 were successively placed into a transparent vessel with a graduated scale, after which quartz particles 2 mm in diameter were added to the samples. The particle settling time was recorded, and the settling rate was subsequently calculated. The results showed that in the PAM-based hydraulic fracturing fluid with a concentration of 3 l/m^3, which exhibited the lowest elastic properties (relaxation time of 12 s), the particle settling rate was 3.0 mm/s. For the sample with a concentration of 5 l/m^3 (relaxation time of 50 s), the settling rate was 1.5 mm/s. For the sample with the highest concentration of 9 l/m^3 (relaxation time of 110 s), the settling rate was 0.8 mm/s. Thus, it was determined that increasing the elastic properties of the hydraulic fracturing fluid improves its proppant transport capacity.

Study [10] compared the settling rate of ceramic proppant in a PAM-based hydraulic fracturing fluid and in a linear gel lacking elastic properties. The loadings of the linear gel and PAM were selected based on equal active substance concentrations: PAM – 6 l/m^3, linear gel – 3 kg/m^3. The samples were prepared using the mineralized water of the Bakken formation at a temperature of 21 °C. The proppant mesh sizes were 20/25 and 60/70. The results of proppant particle settling rate determination under static conditions showed that the PAM-based hydraulic fracturing fluid better retained both the small-mesh proppant (60/70: PAM – 0.025 mm/s, linear gel – 0.064 mm/s) and the large-mesh proppant (20/25: PAM – 0.339 mm/s, linear gel – 4.899 mm/s). Notably, the increase in settling rate in the linear gel upon switching to the larger-mesh proppant was significantly greater than that in the PAM-based hydraulic fracturing fluid.

Similar studies were conducted in [11] using a sample of quartz sand with mesh sizes of 40 and 70 and a concentration of 60 kg/m^3. The experiment employed an anionic PAM-based hydraulic fracturing fluid with a loading of 4 l/m^3 and a linear gel with a loading of 3 kg/m^3, prepared in distilled water at a temperature of 25 °C. In the linear gel, which lacks elastic properties, the settling rate was 0.08 mm/s for the 40 mesh size and 4.2 mm/s for the 70 mesh size. For the PAM-based hydraulic fracturing fluid, the corresponding values were 0.05 and 0.17 mm/s, respectively.

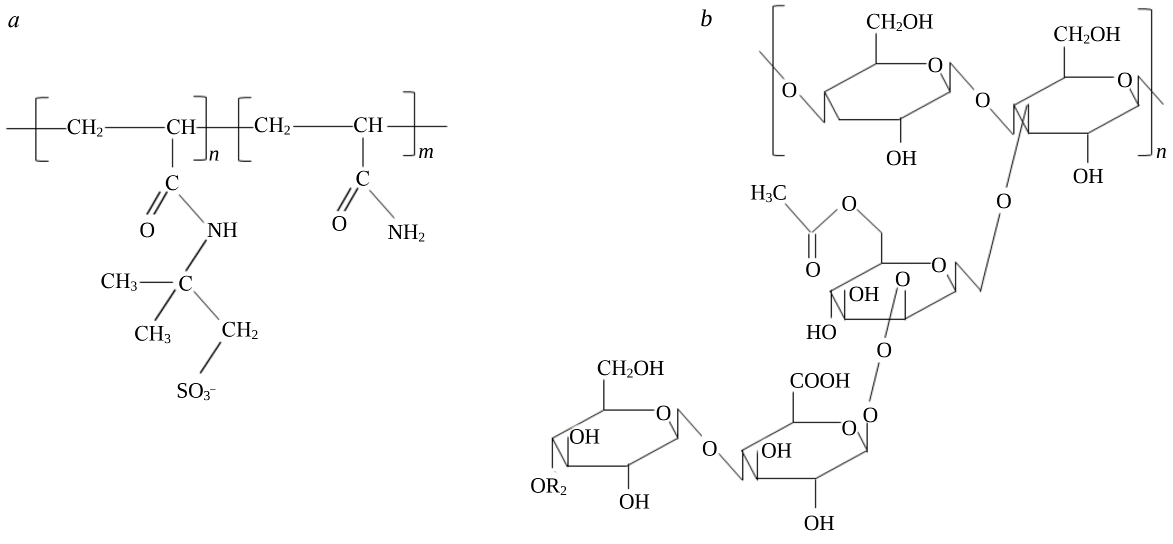

Fig.1. Chemical structure of hydrolyzed PAM (*a*) and guar gum (*b*)

Thus, the conducted studies have demonstrated the significant influence of elastic properties on the proppant transport capacity of hydraulic fracturing fluids, as well as the potential of using PAM as a gelling agent. However, no fundamental analysis has been performed regarding the mechanism by which elastic properties affect the ability of the fluid to suspend and transport proppant.

The aim of this study is to provide a fundamental substantiation of the influence of viscoelastic properties on proppant transport efficiency by employing oscillatory shear testing with periodic recording of amplitude and frequency. This work contains an analysis of Russian and international scientific and technical literature on the research and application of PAM-based viscoelastic fluids, as well as the methodology and results of laboratory studies conducted on a sample of a synthetic polymer and a linear guar gel.

Methods

Viscoelastic fluids are non-Newtonian systems that combine the properties of both liquids and solid (elastic) bodies. At low shear rates, the internal structure of viscoelastic fluids consists of a network of molecules with multidimensional chains folded into disordered coils, which characterize the optimal energy distribution within the chain [12, 13]. An increase in shear rate leads to conformational changes in the polymer molecules, causing them to stretch and redistribute within the fluid volume [14].

The deformation of the molecular structure of the polymer chain is described by Hooke's law:

$$\gamma(t) = \gamma_0 \sin(\omega t), \tag{1}$$

where $\gamma(t)$ is the time-dependent strain, m^{-1}; γ_0 is the strain amplitude, m^{-1}; ω is the angular velocity, s^{-1}; t is the time, s.

The shear stress also follows a sinusoidal function with an additional phase angle shift:

$$\sigma(t) = \sigma_0 \sin(\omega t - \delta), \tag{2}$$

where $\sigma(t)$ is the time-dependent shear stress, Pa; σ_0 is the shear stress amplitude, Pa; δ is the phase angle, rad.

Expressions (1) and (2) characterize the inertia of the deformation process of a body due to the action of elastic forces: when a shear load is applied, full deformation of the molecules occurs after a transient process characterized by a phase angle shift δ between the shear stress and the strain of the body [15]. Depending on the magnitude of the phase angle δ, the behavior of the body can be described by two limiting cases:

- $\delta = 0$, the shear stress in the body is in phase with the applied load. This case characterizes a perfectly elastic body, in which all stored energy is consumed on molecular deformation without losses due to viscous flow;
- $\delta = \pi/2$, the shear stress in the sample is out of phase with the applied load (i.e., in antiphase); this case characterizes a perfectly viscous body, in which all energy is dissipated as viscous flow.

By analyzing the behavior of perfectly viscous and perfectly elastic bodies, it can be concluded that a viscoelastic fluid represents an intermediate state of matter, capable of recovering part of its internal structure through the energy stored by elastic deformations of the polymer molecules, while the remaining energy is dissipated as viscous flow [16].

In studies [17-19] a method was proposed for describing the viscous and elastic components using specific dynamic moduli: the storage modulus G', which characterizes the recovery of the structure after removal of shear stress due to the energy stored as elastic deformation of the polymer molecules; and the loss modulus G'', which characterizes the energy dissipated as viscous flow under shear load.

Based on these statements and Hooke's law, the storage modulus G' can be expressed as a function of the cosine of the phase angle δ, with an argument equal to the ratio of the stress amplitude to the strain amplitude of the body. The loss modulus G'' is described by a function of the sine of the phase angle δ, which is out of phase with the storage modulus G', with an analogous argument. Thus, the storage and loss moduli can be expressed as:

$$\begin{cases} G' = \dfrac{\sigma_0}{\gamma_0}\cos\delta, \\ G'' = \dfrac{\sigma_0}{\gamma_0}\sin\delta. \end{cases} \tag{3}$$

It is evident that the sum of the energy stored through elastic deformation of the polymer molecules and the energy dissipated during viscous flow characterizes the overall rheological behavior of viscoelastic fluids [20]. By transforming into a polar coordinate system and representing the storage and loss moduli as the real and imaginary parts of a complex number, the complex shear modulus parameter of the viscoelastic fluid can be obtained:

$$G^* = \frac{\sigma_t}{\gamma_t} = \frac{\sigma_0}{\gamma_0}e^{i\delta} = \frac{\sigma_0}{\gamma_0}\left(\cos\delta + i\sin\delta\right) = G' + iG''. \tag{4}$$

In turn, the complex shear modulus is related to the complex viscosity by the following formula

$$\mu^* = G^*/\omega, \tag{5}$$

where μ^* is the complex viscosity of the viscoelastic fluid, Pa·s.

From equation (5), an increase in the viscoelastic properties of the fluid leads to an increase in the complex viscosity of the system. However, the question of correctly quantifying the contribution of the viscous and elastic components to the rheology of hydraulic fracturing fluids remains relevant [21, 22]. Rheometers used to evaluate effective viscosity, operating at atmospheric pressure, are incapable of determining the viscoelastic properties of a fluid. To do so, it is necessary to generate multiple changes in shear stress amplitude or frequency over a short period of time to calculate the shift of the response curve relative to the applied shear rate, which cannot be achieved with atmospheric rheometers [23, 24].

To assess the contribution of elastic and viscous properties in hydraulic fracturing fluids, rheometers with an oscillation function are used, such as the HR-3 (Discovery), Rheotest RN 5.3, or Anton Paar instruments. These devices employ a methodology based on subjecting the sample to controlled oscillations at a specified frequency and amplitude [25]. This approach makes it possible to evaluate the viscoelastic characteristics of a material under optimal conditions while preserving the structural integrity of the sample during determination of its dynamic properties. It also reveals behavioral features that do not manifest in constant shear rate tests [26].

To determine the storage modulus G' and loss modulus G'' using an oscillatory rheometer, harmonic strain oscillations are applied. The elastic storage modulus G' characterizes the strain energy stored in the system and reflects the solid-like characteristics of the sample, whereas the viscous loss modulus G'' represents energy dissipation, imparting liquid-like properties to the sample. Thus, the deviation in the interval $0 \le t \le \delta$ quantitatively determines the magnitude of the storage modulus G', while the deviation in the interval $\delta \le t \le \pi/2$ determines the magnitude of the loss modulus G'' [27].

Oscillatory testing is performed in two modes: amplitude sweep (varying the oscillation amplitude at a fixed frequency) and frequency sweep (varying the oscillation frequency at a fixed amplitude) [28].

Amplitude sweep tests allow the region of reversible elastic deformations (LVE range) to be assessed, i.e., the range of strain amplitudes within which the tested sample maintains structural stability as the applied load increases (Fig.2, *a*). In Fig.2, *b*, the LVE range is characterized by the parallelism of the G' and G'' curves relative to the strain axis Y. When the dynamic moduli G' and G'' deviate from parallel values, irreversible disruption of the polymer structure begins to occur in the system, during which the energy of elastic deformations starts to be dissipated as viscous friction, as demonstrated by the gradual convergence of the G' and G'' curves. The intersection point of the G' and G'' lines is quantitatively equal to the static shear stress, above which the sample irreversibly loses its elastic properties. Based on this, conclusions can be drawn regarding the behavior of the fluid depending on the values of the storage modulus G' and loss modulus G'': when $G' > G''$, the sample corresponds to a viscoelastic fluid; when $G' < G''$, it corresponds to a viscous fluid.

Frequency sweep tests are used to evaluate the viscoelastic properties of fluids under nonstationary shear loading conditions (Fig.2, *c*). The dependences of G' and G'' are logarithmic in nature, and at their intersection point, the accumulated energy from elastic deformations and the dissipated energy are equal. The reciprocal of the angular frequency ω at which the intersection of G' and G'' occurs is called the relaxation time λ. An increase in the relaxation time λ of the fluid indicates a greater amount of energy stored through elastic deformation of chain segments and, consequently, more pronounced elastic properties. Accordingly, the lower the deformation frequency at which the intersection of the dynamic moduli G' and G'' occurs, the more pronounced the elastic properties of the sample (Fig.2, *d*).

In addition to the storage and loss moduli, the first normal stress difference N_1 can be determined using oscillatory rheometers. The physical meaning of the first normal stress difference lies in the generation of normal components in the stress tensor of fluids with elastic polymer chains. During shear flow of purely viscous fluids, only shear stresses act in the medium, since the bonding forces between molecules within the fluid volume are negligibly small. When polymer molecules are added to the fluid, interactions between the formed molecular coils are initiated, and with increasing polymer concentration, the intermolecular interaction intensifies to the point of chain entanglement [29].

The behavior of viscoelastic fluids is described by the Weissenberg effect, according to which, when a rod is rotated at a given angular velocity, the fluid is not thrown toward the vessel walls due to centripetal acceleration, forming a vortex around the rod; instead, it adheres to the rod surface due to mutual molecular entanglement. The force of molecular entanglement is governed by the elastic nature of their bonds, which tends to return the molecule to its original conformational state. As a

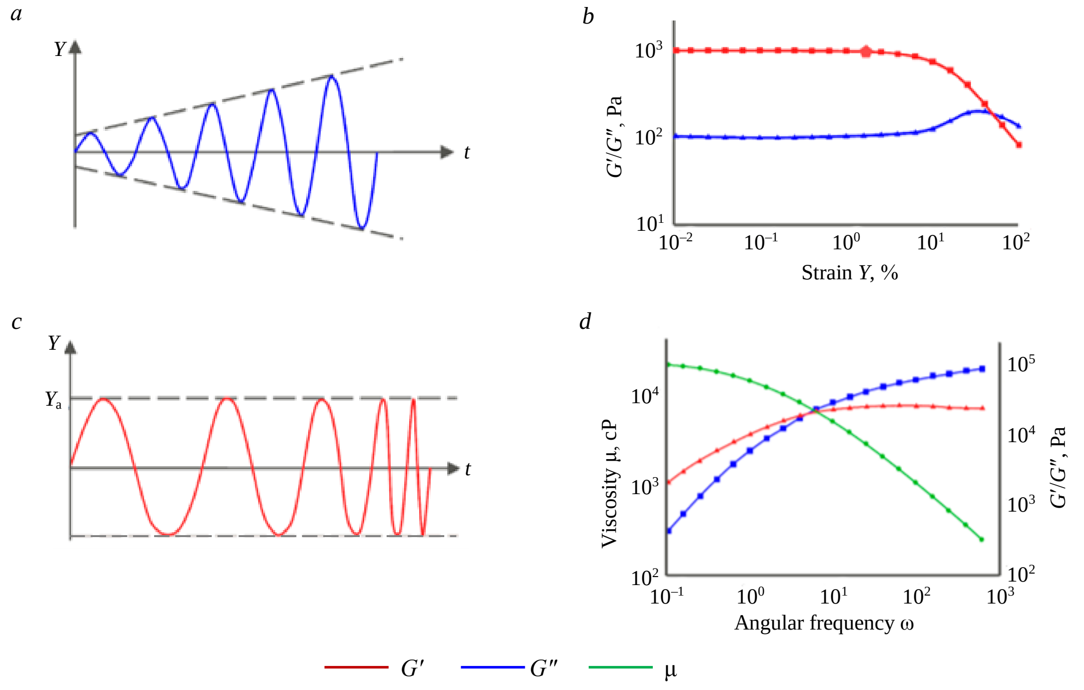

Fig.2. Typical results of oscillatory testing in amplitude sweep (*a*, *b*)
and frequency sweep modes (*c*, *d*)

result, surrounding molecules are captured by the deformed molecules adhered to the rod surface. Consequently, the greater the elasticity of the molecular bonds in the sample, the more pronounced the Weissenberg effect [30]. This mechanism can be described analytically by decomposing the stress state of the conformationally altered molecules into tangential and orthogonal components of the stress deviator (Fig.3). Let a shear deformation stress σ_{11} be applied to a sample element along the *OX* axis. The deformed molecules then tend to return to their original state, which gives rise to normal deformation components σ_{22} and σ_{33} directed along the *OZ* and *OY* axes, respectively. The difference between the normal and tangential stress components within the polymer chains is numerically equal to the first and second normal stress differences:

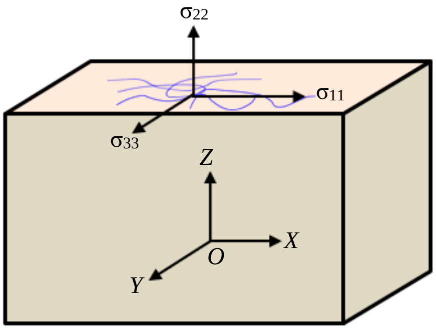

Fig.3. Initiation of stresses in a viscoelastic body element under shear

$$\begin{cases} N_1 = \sigma_{22} - \sigma_{11}, \\ N_2 = \sigma_{33} - \sigma_{11}. \end{cases}$$

The conducted studies have shown that the first normal stress difference N_1 makes a significant contribution to the elastic behavior of hydraulic fracturing fluids, whereas the second normal stress difference N_2 is negligibly small due to the small values of the σ_{33} components.

It is proposed to analytically determine the fundamental relationship between viscoelastic properties and proppant transport efficiency by expanding the classical Stokes formula. The classical Stokes formula, which describes the settling velocity of a solid particle in a fluid, shows that proppant suspension capacity depends on the effective viscosity μ, the density of the system ρ_f, as well as the density ρ_p and diameter d of the suspended particles:

$$v_0 = \frac{2\left(\rho_p - \rho_f\right) d^2 g}{18\mu},$$

where ρ_p is the particle density, kg/m^3; ρ_f is the fluid density, kg/m^3.

Clearly, an increase in fluid viscosity improves proppant suspension capacity by increasing the drag force exerted by the fluid on the particle:

$$F_{st} = 3\pi\mu U d,$$

where U is the magnitude of the particle velocity relative to the fluid, m/s.

The drag force on the particle can be expressed as an integral over the particle surface Ω:

$$F_{st} = \int nT' dS,$$

where n is the unit normal vector to the surface; T' is the stress tensor in the fluid, Pa; S is the surface area of the particle, m^2.

The stress tensor in the fluid can be decomposed into the viscous stress tensor K' and the product of the absolute pressure P and the identity matrix I':

$$T' = -PI' + K'.$$

Upon further expansion of the viscous stress tensor K', it can be shown that its magnitude depends on both the effective viscosity of the system and the strain rate tensor:

$$\begin{cases} K' = 2\mu S' - \frac{2}{3}\mu\left(\nabla u\right) I', \\ S' = \frac{1}{2}\left(\nabla u + \left(\nabla u\right)^T\right), \end{cases}$$

where u is the velocity field; S' is the strain rate tensor, s^{-1}.

Thus, it has been determined that the elastic properties of the fluid, which characterize the energy stored through elastic deformations, are a component of the total stress tensor within the viscous stress tensor and are independent of the effective viscosity of the fluid. This circumstance accounts for the influence of elastic properties on the particle settling rate in hydraulic fracturing fluids and their significance when using low-viscosity fluids. At a given flow rate, the flow regime in a fracture for a high-viscosity fluid is laminar, whereas for a low-viscosity fluid it is turbulent. The transition of the fluid flow to turbulence has a positive effect on proppant transport in the fracture [31]. In this regard, the use of low-viscosity hydraulic fracturing fluids is the most promising approach to improving the cost-effectiveness of hydrocarbon production from reservoirs with hard-to-recover reserves.

Results and discussion

Laboratory studies to evaluate viscoelastic properties were conducted on a sample of anionic PAM-based hydraulic fracturing fluid in the form of a suspension using an Anton Paar MCR 702 TwinDrive oscillatory rheometer in frequency sweep mode. The primary parameter of interest was the relaxation time λ. The oscillation frequency range was 0.2-30 Hz, and the test temperature was 25 °C. To identify the advantages of using low-viscosity synthetic hydraulic fracturing fluids, an equivalent set of tests was performed on a linear guar gel sample under identical thermobaric conditions. The polymer loading for the linear guar gel was 2 kg/m^3, in accordance with the practice of high-hydraulic fracturing in low-permeability terrigenous reservoirs of Western Siberia (see Table). Accordingly, based on equal active substance concentrations in the tested solutions, the polymer loading for the PAM-based hydraulic fracturing fluid, supplied in suspension form, was 4 l/m^3.

Geological and physical parameters of low-permeability reservoirs in Western Siberia (average values for all formations)

Formation group	Permeability, mD	Porosity, fraction	Effective oil-saturated thickness, m	Net-to-gross ratio, fraction
AS	1.68	0.17	12.7	0.43
Ach	1.56	0.16	15.2	0.30
YuS	1.48	0.14	9.6	0.21

Each sample was placed into the measuring cell of the rheometer. The temperature was then set to 25 °C and the oscillation amplitude to 40 %, both of which were maintained constant throughout the study. In accordance with the instrument operating manual, after setting the test mode and starting the rheometer, the polymer samples were subjected to an oscillatory shear load, starting from the maximum value. The rheometer's sensitive elements recorded the change in polymer deformation, yielding the values of the storage modulus G' and loss modulus G'' at each specified time point. A total of 13 measurements were recorded for each sample over the entire oscillation frequency range, based on which the corresponding graphs were constructed (Fig.4).

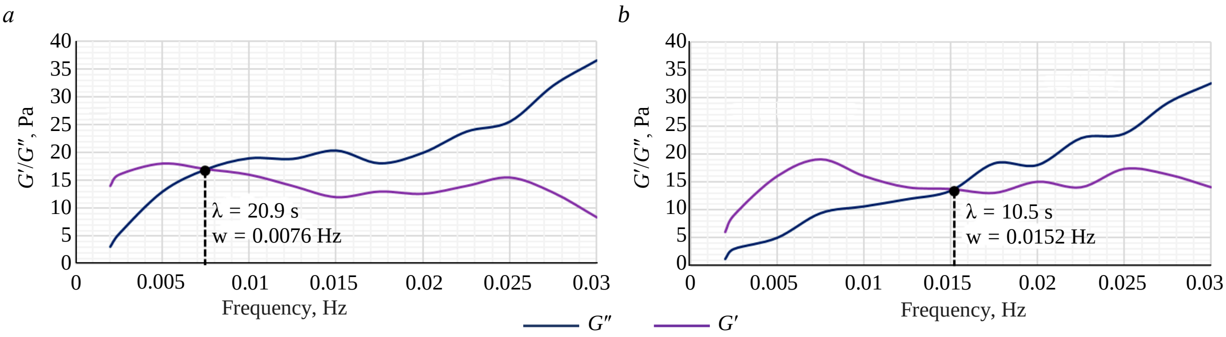

Fig.4. Results of storage modulus G' and loss modulus G'' measurements for PAM-based hydraulic fracturing fluid (*a*) and linear guar gel (*b*) in frequency sweep mode (T = 25 °C)

Based on the obtained results, it was determined that the intersection of the G' and G'' curves occurred at an oscillation frequency of 0.0076 Hz for the PAM-based hydraulic fracturing fluid and at 0.0152 Hz for the linear guar gel. Since the relaxation time λ is inversely proportional to twice the product of the oscillation frequency and π, the relaxation time λ for the PAM-based hydraulic fracturing fluid was 20.9 s, whereas for the linear guar gel it was 10.5 s. Thus, the relaxation time λ of the synthetic PAM-based fluid was 1.99 times greater than that of the linear guar gel.

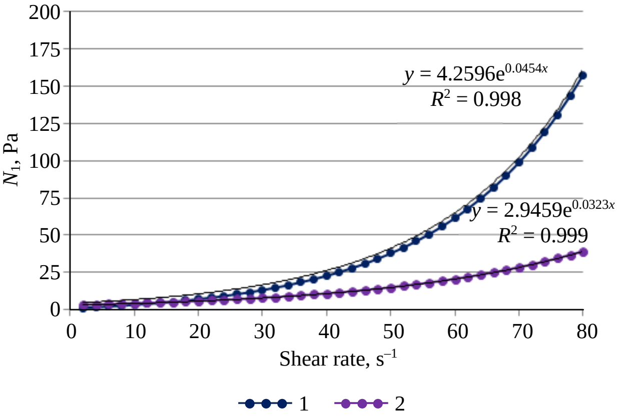

Fig.5. Results of first normal stress difference N_1 measurements for PAM-based hydraulic fracturing fluid (1) and linear guar gel (2)

The first normal stress difference N_1 was evaluated similarly using an Anton Paar MCR 702 TwinDrive oscillatory rheometer in steady-state flow mode with a progressive increase in shear rate from 1 to 80 s^{-1}. A total of 40 measurements were taken for each hydraulic fracturing fluid sample, followed by the construction of the corresponding graphs (Fig.5).

Based on the obtained results, the following observations can be made:

- the first normal stress difference N_1 increases exponentially with increasing shear rate for both samples;
- for the synthetic hydraulic fracturing fluid, the first normal stress difference N_1 is more than four times higher than that of the linear guar gel – 157.4 Pa and 39.2 Pa, respectively, at a shear rate of 80 s^{-1}.

The greatest difference in N_1 values is observed at high shear rates, indicating that elastic properties have the most pronounced influence on hydraulic fracturing fluid behavior under high shear loads [32]. In reservoir conditions during fracture propagation, this feature of viscoelastic synthetic hydraulic fracturing fluids allows the proppant to remain suspended longer, preventing its premature settling near the wellbore [33-35]. Clearly, for hydraulic fracturing purposes, increasing the viscoelastic properties of the treatment fluid is advantageous, as it enables the use of low-viscosity systems as friction reducers to enhance the stimulated reservoir volume.

Thus, based on the results of the conducted viscoelastic property evaluation studies, it has been demonstrated that a PAM-based hydraulic fracturing fluid at comparable active substance concentrations exhibits more pronounced elastic properties – characterized by relaxation time λ and first normal stress difference N_1 – than a linear guar gel.

To establish a relationship between viscoelastic properties and the proppant transport capacity of hydraulic fracturing fluids, laboratory studies were also conducted to evaluate the proppant settling rate.

The elastic deformations of the denser molecular chains of PAM can store a larger portion of the energy expended during fluid injection than guar gels. The energy stored in this way preserves the internal spatial structure of the fluid, which positively affects the transport and suspension of the proppant. In other words, a longer molecular deformation, where the relaxation time λ is comparable to the time required for a proppant particle to travel a distance *dz*, creates resistance to particle motion, resulting in prolonged proppant settling even at low hydraulic fracturing fluid viscosity. The low viscosity of synthetic systems makes it possible to reduce the pressure inside the fracture, promoting fracture growth in length while limiting height growth, as well as to reduce operating costs associated with fluid cleanup after hydraulic fracturing.

Prior to conducting the laboratory study on proppant suspension capacity, the effective viscosity of the PAM-based fluid and the linear gel was evaluated using a Fann 35 rotational viscometer

Fig.6. Fann 35 atmospheric rotational viscometer

(Fig.6). At a shear rate of 100 s^{-1}, the effective viscosity of the PAM-based hydraulic fracturing fluid was 14 cP for a concentration of 2 l/m^3 and 36 cP for a concentration of 4 l/m^3. The effective viscosity of the linear guar gel at a shear rate of 100 s^{-1} was 36 and 78 cP, respectively.

The obtained results showed that the effective viscosity of the PAM-based hydraulic fracturing fluid is 2.2-2.6 times lower compared to that of the linear gel at comparable polymer concentrations. Given that the average molecular weight of polyacrylic acid (a derivative for all types of PAM) is 72.06 g/mol, while the molecular weight of guar gels, due to their complex polymer structure with long β-glycosidic bonds, reaches values of 180.16 g/mol and higher, the obtained results demonstrate a direct influence of the chemical structure and molecular size of the polymer on the overall viscosity of the system. It can be concluded that, due to the substantially smaller size of PAM molecules, the density of polymer bonds in synthetic fluids is significantly higher than that in guar gels without a crosslinker. This finding explains the origin of the more pronounced elastic properties of PAM-based synthetic hydraulic fracturing fluids compared to linear gels.

Subsequently, laboratory studies of proppant settling rate under static conditions were conducted for PAM-based hydraulic fracturing fluid and linear gel samples prepared in distilled water at a temperature of 25 °C at two polymer concentrations: 2 and 4 l/m^3 for the synthetic polymer, and 1.8 and 4.2 kg/m^3 for the linear gel. ForeProp ceramic proppant of 16/20 mesh size at a concentration of 700 kg/m^3 was used as the proppant.

For the study, graduated vessels were used, into which 100 mL of freshly prepared polymer was placed with the addition of proppant at a concentration of 700 kg/m^3. Immediately after placing the mixture into the vessel, a stopwatch was started. At 5, 30, and 120 min, the portion of the total proppant volume that had settled to the bottom of the graduated vessel was visually assessed for each test sample. The determination of the proppant suspension capacity of the hydraulic fracturing fluids yielded the following results:

- the proppant settling time in the PAM-based hydraulic fracturing fluid at polymer concentrations of 2 and 4 l/m^3 was 120 and 960 min, respectively;
- the proppant settling time in the linear gel at polymer concentrations of 1.8 and 4.2 kg/m^3 was 5 and 30 min, respectively.

Based on the obtained results, it was concluded that the settling rate of 16/20 mesh ceramic proppant in the PAM-based hydraulic fracturing fluid was 24 times lower than that in the linear gel at a concentration of 2 l/m^3 (0.2 mm/s and 4.83 mm/s, respectively) and 32 times lower at a concentration of 4 l/m^3 (0.03 mm/s and 0.96 mm/s, respectively) under static conditions (Fig.7).

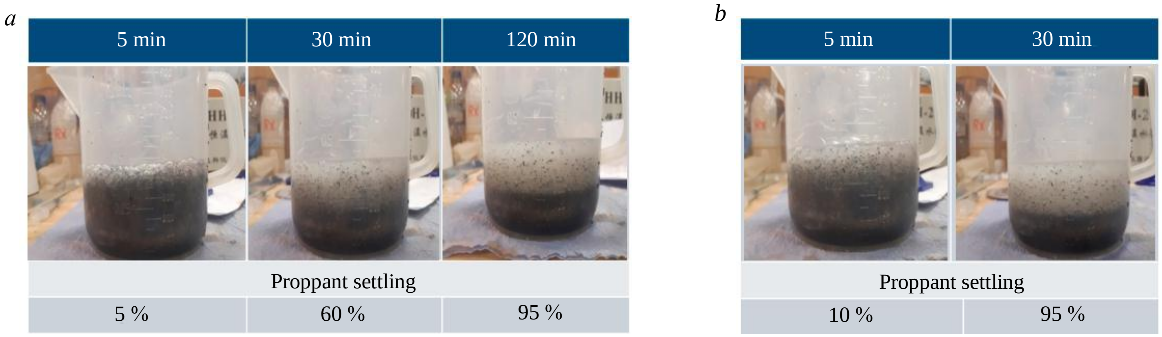

Fig.7. Proppant particle settling time in anionic PAM-based fluid (*a*) and linear guar gel (*b*) under static conditions

Given that the linear gel, as determined earlier, has significantly lower viscoelastic properties than the synthetic polymer, it can be concluded that the increased proppant suspension capacity of PAM-based fluids is directly related to their more pronounced elasticity, which compensates for the loss of fluid viscosity over time and under external loading.

Conclusion

Recent trends, characterized by a rapid increase in hydraulic fracturing operations in unconventional reservoirs with extremely poor porosity and permeability properties, as well as a gradual transition from standard crosslinked guar gel fracturing designs to hybrid designs and those employing polyacrylamide-based friction reducers, underscore the relevance of the problem of determining the influence of viscoelastic properties of synthetic hydraulic fracturing fluids on their proppant transport capacity.

The conducted study is aimed at providing a fundamental substantiation of the influence of viscoelastic properties of hydraulic fracturing fluids on the efficiency of proppant transport and retention. Early approaches to assessing proppant transport capacity asserted that fluid viscosity plays a key role in proppant retention; however, the results of the conducted studies confirm the significant influence of the elastic properties of the polymer system on proppant transport capacity, particularly when using low-viscosity synthetic fluids based on polyacrylamide.

The analysis of the nature of viscoelastic behavior of polymer fluids, along with the results of the conducted laboratory studies, has led to the following conclusions:

- PAM-based hydraulic fracturing fluids have significantly lower effective viscosity compared to guar gels (by a factor of 2.2-2.6), which is due to the lower molecular weight and smaller molecular size of the synthetic polymers compared to linear guar gels;
- the relaxation time λ for the synthetic PAM-based hydraulic fracturing fluid was 20.9 s, which is 1.99 times greater than that of the linear guar gel (10.5 s);
- the higher values of first normal stress difference N_1 (4 times higher at a shear rate of 80 s^{-1}) and relaxation time λ indicate more efficient formation of elastic forces that resist proppant settling;
- laboratory studies of proppant settling under static conditions showed that the particle settling time in the PAM-based hydraulic fracturing fluid reaches 120 and 960 min at concentrations of 2 and 4 l/m^3, respectively, whereas for the linear gel this parameter is 5 and 30 min at comparable active substance concentrations. Thus, the proppant settling rate in the synthetic hydraulic fracturing fluid was 24-32 times lower than that in the linear guar gel.

The conducted studies have provided both theoretical and experimental substantiation of the effectiveness of using low-viscosity PAM-based hydraulic fracturing fluids, which possess pronounced viscoelastic properties, for the purpose of enhancing hydrocarbon production from reservoirs with low porosity and permeability. Due to their improved elastic characteristics, synthetic fluids ensure effective proppant retention throughout the entire half-length of the hydraulic fracture despite lower system viscosity, which promotes increased fracture length and reduces the risk of vertical fracture breakthrough into overlying or underlying water-saturated interlayers. The low viscosity of PAM-based hydraulic fracturing fluids facilitates subsequent fluid cleanup from the near-wellbore zone, reducing operating costs and minimizing the risk of near-wellbore formation damage due to reaction products with reservoir fluids.

Thus, the study confirms the promise of transitioning from high-viscosity gels to viscoelastic low-viscosity PAM-based systems, opening new opportunities for technologically efficient and cost-effective development of hard-to-recover hydrocarbon reserves.

REFERENCES

1. Al-Hajri S., Negash B.M., Rahman M.M. et al. Perspective Review of Polymers as Additives in Water-Based Fracturing Fluids. *ACS Omega*. 2022. Vol. 7. Iss. 9, p. 7431-7443. DOI: 10.1021/acsomega.1c06739

2. Sadykov A.M., Sirbaev R.I., Erastov S.A. et al. The influence of various hydraulic fracturing fluids on the residual conductivity of the proppant pack and the filtration properties of low–permeability reservoirs. *Oil Industry*. 2023. N 7, p. 52-57 (in Russian). DOI: 10.24887/0028-2448-2023-7-52-57

3. Feng Liang, Al-Muntasheri G., Ow H., Cox J. Reduced-Polymer-Loading, High–Temperature Fracturing Fluids by Use of Nanocrosslinkers. *SPE Journal*. 2017. Vol. 22. Iss. 2, p. 622-631. DOI: 10.2118/177469-PA

4. Skauge A., Zamani N., Jacobsen J.G. et al. Polymer Flow in Porous Media: Relevance to Enhanced Oil Recovery. *Colloids and Interfaces*. 2018. Vol. 2. Iss. 3. N 27. DOI: 10.3390/colloids2030027

5. Yang Zhang, Shuyue Xiao, Jincheng Mao et al. Construction of a Novel Fracturing Fluid with High Viscoelasticity Induced by Mixed Micelles. *SPE Journal*. 2023. Vol. 28. Iss. 4, p. 2080-2093. DOI: 10.2118/214670-PA

6. Rock A., Hincapie R.E., Tahir M. et al. On the Role of Polymer Viscoelasticity in Enhanced Oil Recovery: Extensive Laboratory Data and Review. *Polymers*. 2020. Vol. 12. Iss. 10. N 2276. DOI: 10.3390/polym12102276

7. Shengming Huang, Guancheng Jiang, Zilun Chang et al. Investigation of Novel Modified Nanoparticle–Enhanced Viscoelastic Surfactant Clean Fracturing Fluid System for Improving Oil Recovery in Low-Permeability Reservoirs. *SPE Journal*. 2025. Vol. 30. Iss. 11, p. 7177-7191. DOI: 10.2118/230307–PA

8. Shenglong Shi, Jinsheng Sun, Kaihe Lv et al. Comparative Studies on Thickeners as Hydraulic Fracturing Fluids: Suspension versus Powder. *Gels*. 2022. Vol. 8. Iss. 11. N 722. DOI: 10.3390/gels8110722

9. Biheri G., Imqam A. Proppant Transport Using High-Viscosity Friction Reducer Fracture Fluids at High-Temperature Environment. *SPE Journal*. 2022. Vol. 27. Iss. 1, p. 60-76. DOI: 10.2118/206750-PA

10. Singh A., Xinghui Liu, Jiehao Wang, Rijken M.C.M. Novel Learnings of Proppant Transport Behavior in Unconventional Hydraulic Fractures. *SPE Journal*. 2022. Vol. 27. Iss. 5, p. 2980-3000. DOI: 10.2118/204135-PA

11. Tomomewo O.S., Mann M., Anyim L. et al. Maximizing the Proppant Carrying and Viscoelastic Properties of the Bakken Hypersaline-Produced Water with High-Viscosity Friction Reducers for Sustainable Applications. *SPE Journal*. 2022. Vol. 27. Iss. 6, p. 3688-3703. DOI: 10.2118/200809-PA

12. Zeynalli M., Al-Shalabi E.W., Waleed A. An Extended Unified Viscoelastic Model for Predicting Polymer Apparent Viscosity at Different Shear Rates. *SPE Reservoir Evaluation & Engineering*. 2023. Vol. 26. Iss. 1, p. 99-121. DOI: 10.2118/206010-PA

13. Costanzo S., Qian Huang, Ianniruberto G. et al. Shear and Extensional Rheology of Polystyrene Melts and Solutions with the Same Number of Entanglements. *Macromolecules*. 2016. Vol. 49. Iss. 10, p. 3925-3935. DOI: 10.1021/acs.macromol.6b00409

14. Lotfollahi M., Farajzadeh R., Delshad M. et al. Mechanistic Simulation of Polymer Injectivity in Field Tests. *SPE Journal*. 2016. Vol. 21. Iss. 4, p. 1178-1191. DOI: 10.2118/174665-PA

15. Alotaibi M.A., Miskimins J. Slickwater Proppant Transport in Hydraulic Fractures: New Experimental Findings and Scalable Correlation. *SPE Production & Operations*. 2018. Vol. 33. Iss. 2, p. 164-178. DOI: 10.2118/174828-PA

16. Azad M.S. Characterization of Nonlinear Viscoelastic Properties of Enhanced Oil Recovery Polymer Systems Using Steady-Shear Rheometry. *SPE Journal*. 2023. Vol. 28. Iss. 2, p. 664-682. DOI: 10.2118/212824-PA

17. Åsen S.M., Stavland A., Strand D., Hiorth A. An Experimental Investigation of Polymer Mechanical Degradation at the Centimeter and Meter Scale. *SPE Journal*. 2019. Vol. 24. Iss. 4, p. 1700-1713. DOI: 10.2118/190225-PA

18. Costanzo S., Ianniruberto G., Marrucci G., Vlassopoulos D. Measuring and assessing first and second normal stress differences of polymeric fluids with a modular cone-partitioned plate geometry. *Rheologica Acta*. 2018. Vol. 57. Iss. 5, p. 363-376. DOI: 10.1007/s00397-018-1080-1

19. Xiaojing Ge, Imqam A. Laboratory Comparative Study of Anionic and Cationic High-Viscosity Friction Reducers in Moderate to Extremely High Total Dissolved Solids Environments. *SPE Journal*. 2023. Vol. 28. Iss. 2, p. 876-893. DOI: 10.2118/212298-PA

20. Kulichikhin V.G., Malkin A.Ya., Frenkin E.I., Semakov A.V. Measurement of Viscoelastic Characteristics of Interfacial Layers on Liquid Surfaces Using New Experimental Equipment. *Colloid Journal*. 2019. Vol. 81. N 6, p. 681-686. DOI: 10.1134/S1061933X19060097

21. Arnipall S.K., Ergun K. Settling Velocity of Particles in Viscoelastic Fluids: A Comparison of the Shear-Viscosity and Elasticity Effects. *SPE Journal*. 2018. Vol. 23. Iss. 5, p. 1689-1705. DOI: 10.2118/187255-PA

22. Azad M.S., Japan J.T. Extensional Effects during Viscoelastic Polymer Flooding: Understanding Unresolved Challenges. *SPE Journal*. 2020. Vol. 25. Iss. 4, p. 1827-1841. DOI: 10.2118/201112-PA

23. Silin M.A., Magadova L.A., Krisanova P.K. et al. Possibilities of oscillation testing in field chemistry. *Oil Industry*. 2024. N 4, p. 97-102 (in Russian). DOI: 10.24887/0028-2448-2024-4-97-102

24. Loginova M.Ye., Agzamov F.A., Ismakov R.A. Investigation of viscoelastic properties of buffer fluids to improve the quality of well anchoring. *Industrial Production and Use Elastomers*. 2022. N 3-4, p. 39-48 (in Russian). DOI: 10.24412/2071-8268-2022-3-4-39-48

25. McCormack K.L., McLennan J.D., Jagniecki E.A., McPherson B.J. Discrete Measurements of the Least Horizontal Principal Stress from Core Data: An Application of Viscoelastic Stress Relaxation. *SPE Reservoir Evaluation & Engineering*. 2023. Vol. 26. Iss. 3, p. 827-841. DOI: 10.2118/214669-PA

26. Zhenming Xu, Xianzhi Song, Zhaopeng Zhu. Development of Elastic Drag Coefficient Model and Explicit Terminal Settling Velocity Equation for Particles in Viscoelastic Fluids. *SPE Journal*. 2020. Vol. 25. Iss. 6, p. 2962-2983. DOI: 10.2118/201194-PA

27. Tao Lin Sun, Feng Luo, Wei Hong et al. Bulk Energy Dissipation Mechanism for the Fracture of Tough and Self-Healing Hydrogels. *Macromolecules*. 2017. Vol. 50. Iss. 7, p. 2923-2931. DOI: 10.1021/acs.macromol.7b00162

28. Zare Y., Rhee K.Y. Expression of normal stress difference and relaxation modulus for ternary nanocomposites containing biodegradable polymers and carbon nanotubes by storage and loss modulus data. *Composites Part B: Engineering*. 2019. Vol. 158, p. 162-168. DOI: 10.1016/j.compositesb.2018.09.076

29. Kazemi A., Norouzi M., Nejad A.A. et al. An experimental study on the role and contribution of the first normal stress difference and elongational viscosity in immiscible viscoelastic Saffman-Taylor instability. *Chemical Engineering Research and Design*. 2023. Vol. 197, p. 211-227. DOI: 10.1016/j.cherd.2023.07.036

30. Xiaojing Ge, Imqam A. How Anions and Cations Impact the Viscosity and Viscoelasticity of High-Viscosity Friction Reducers. *SPE Journal*. 2024. Vol. 29. Iss. 2, p. 1076-1090. DOI: 10.2118/218009-PA

31. Kashapov D.V., Shakirov L.R. Mathematical modeling of proppant settling in a horizontal well during hydraulic fracturing operation on a low-viscosity fluid. *Burenie i neft*. 2021. N 7-8, p. 60-65 (in Russian).

32. Rixing Zhang, Nasr-El-Din H., Xiaochun Jin et al. Multiscale Investigation of a Less-Damaging Friction Reducer to Mitigate Formation Damage in Unconventional Shale Reservoirs. *Improved Oil and Gas Recovery*. 2019. Vol. 3, p. 18. DOI: 10.14800/IOGR.455

33. Hai Qu, Yang Xu, Jun Hong et al. Experimental and Visual Analysis of Proppant-Slickwater Flow in a Large-Scaled Rough Fracture. *SPE Journal*. 2023. Vol. 28. Iss. 2, p. 477-495. DOI: 10.2118/212283-PA

34. Hang Xu, Fujian Zhou, Hao Wu et al. Experimental Research on the Proppant Settling and Transport Characteristics of Silica Gel-Based Fracturing Fluid. *SPE Journal*. 2024. Vol. 29. Iss. 3, p. 1321-1336. DOI: 10.2118/218381-PA

35. Kolle J.J., Mueller A.C., Baumgartner S., Cuthill D. Modeling Proppant Transport in Perforated Casing Based on Surface Testing. *SPE Drilling & Completion*. 2023. Vol. 38. Iss. 2, p. 358-369. DOI: 10.2118/209178-PA

Authors**: Dinis V. Imangulov,** *Postgraduate Student* (*Ufa State Petroleum Technological University*, *Ufa*, *Republic of Bashkortostan*, *Russia*), *dinis.imangulov@gmail.com*, *https://orcid.org/0000-0002-8984-7974*, **Aleksandr I. Ponomarev,** *Doctor of Engineering Sciences*, *Professor* (*Ufa State Petroleum Technological University*, *Ufa*, *Republic of Bashkortostan*, *Russia*), *https://orcid.org/0000-0003-0483-7732*, **Denis V. Kashapov,** *Candidate of Engineering Sciences*, *Associate Professor* (*Ufa State Petroleum Technological University*, *Ufa*, *Republic of Bashkortostan*, *Russia*), *https://orcid.org/0000-0001-6467-0191*.

The authors declare no conflict of interests.